Sorcin modulation of Ca^{2+} sparks in rat vascular smooth muscle cells

Angélica Rueda[1], Ming Song[2], Ligia Toro[2], Enrico Stefani[2] and Héctor H. Valdivia[1]

[1]*Department of Physiology, University of Wisconsin Medical School, Madison, WI 53711, USA*
[2]*Department of Anaesthesiology, David Geffen School of Medicine, UCLA, Los Angeles, CA 90095, USA*

Spontaneous, local Ca^{2+} release events or Ca^{2+} sparks by ryanodine receptors (RyRs) are important determinants of vascular tone and arteriolar resistance, but the mechanisms that modulate their properties in smooth muscle are poorly understood. Sorcin, a Ca^{2+}-binding protein that associates with cardiac RyRs and quickly stops Ca^{2+} release in the heart, provides a potential mechanism to modulate Ca^{2+} sparks in vascular smooth muscle, but little is known about the functional role of sorcin in this tissue. In this work, we characterized the expression and intracellular location of sorcin in aorta and cerebral artery and gained mechanistic insights into its functional role as a modulator of Ca^{2+} sparks. Sorcin is present in endothelial and smooth muscle cells, as assessed by immunocytochemical and Western blot analyses. Smooth muscle sorcin translocates from cytosolic to membranous compartments in a Ca^{2+}-dependent manner and associates with RyRs, as shown by coimmunoprecipitation and immunostaining experiments. Ca^{2+} sparks recorded in saponin-permeabilized vascular myocytes have increased frequency, duration and spatial spread but reduced amplitude with respect to Ca^{2+} sparks in intact cells, suggesting that permeabilization disrupts the normal organization of RyRs and releases diffusible substances that control Ca^{2+} spark properties. Perfusion of 2 μM sorcin onto permeabilized myocytes reduced the amplitude, duration and spatial spread of Ca^{2+} sparks, demonstrating that sorcin effectively regulates Ca^{2+} signalling in vascular smooth muscle. Together with a dense distribution in the perimeter of the cell along a pool of RyRs, these properties make sorcin a viable candidate to modulate vascular tone in smooth muscle.

(Resubmitted 22 May 2006; accepted after revision 18 August 2006; first published online 24 August 2006)
Corresponding author H. H. Valdivia: Department of Physiology, University of Wisconsin Medical School, 601 Science Dr Madison, WI 53711, USA. Email: valdivia@physiology.wisc.edu

Ryanodine-sensitive Ca^{2+} release channels (ryanodine receptors or RyRs) in high resistance vascular smooth muscle (VSM) generate local and spontaneous Ca^{2+} release events (Ca^{2+} sparks) that have many similarities to those observed in cardiac muscle (Nelson *et al.* 1995; Jaggar *et al.* 1998; Jaggar *et al.* 2000), but the functional contribution of these Ca^{2+} sparks to the depolarization-induced global rise in intracellular $[Ca^{2+}]$ is not well understood. Summation of individual Ca^{2+} release events in cardiac and skeletal muscle generate global $[Ca^{2+}]_i$ transients that trigger contraction, but Ca^{2+} sparks in vascular smooth muscle cells (VSMCs) appear to be restricted to sites favourable for activation of large conductance Ca^{2+}-activated K^+ channels (BK_{Ca} channels). An appealing hypothesis therefore is that instead of contributing to muscle contraction as it occurs in striated muscle, Ca^{2+} sparks of VSM may facilitate muscle relaxation by causing membrane hyperpolarization and decreasing Ca^{2+} influx by deactivation of voltage dependent L-type Ca^{2+} channels (VDCCs). (Nelson *et al.* 1995; Pérez *et al.* 1999; Jaggar *et al.* 2000).

Sorcin (*so*luble *r*esistance-related *c*alcium binding prote*in*) is a penta-EF hand Ca^{2+}-binding protein that in the heart regulates intracellular Ca^{2+} homeostasis by interacting with proteins involved in excitation–contraction (E-C) coupling such as RyRs (Meyers *et al.* 1995*b*, 2003; Lokuta *et al.* 1997; Farrell *et al.* 2003) and the Na^+–Ca^{2+} exchanger (Seidler *et al.* 2003). Other protein targets continue to emerge (Meyers *et al.* 2003; Suarez *et al.* 2004; Matsumoto *et al.* 2005; Frank *et al.* 2005), placing sorcin as an important molecular switchboard that links Ca^{2+} signals with effector proteins. In all tissues where it is expressed, sorcin is largely soluble at low $[Ca^{2+}]$ (< 1 μM) and supposedly inactive, but at high $[Ca^{2+}]_i$ it undergoes conformational changes that expose hydrophobic residues and trigger binding to membrane-embedded protein targets (Meyers *et al.* 1995*a*; Farrell *et al.* 2003). We have previously shown that sorcin binds with high affinity to

 DOI: 10.1113/jphysiol.2006.113951

single cardiac RyRs and quickly inhibits their activity (Lokuta *et al.* 1997; Farrell *et al.* 2003). In intact mouse cardiomyocytes, sorcin attenuates Ca^{2+} sparks and $[Ca^{2+}]_i$ transients (Farrell *et al.* 2003), acting, therefore, as a candidate to help stop the inherently positive feedback of Ca^{2+}-induced Ca^{2+} release (CICR) in heart (Valdivia, 1998; Stern & Cheng, 2004). Sorcin's role in VSMCs, however, is unknown, and its potential role as regulator of RyR activity, Ca^{2+} signalling and vascular tone has not been determined.

In this study, we characterized the expression, intracellular localization, and Ca^{2+}-dependent translocation of sorcin in vascular smooth muscle tissue, specifically in cerebral artery and aorta, and gained mechanist insight into its functional role as modulator of Ca^{2+} signalling in this tissue. We found that, like in the heart, a pool of VSM sorcin is strategically located in the vicinity of RyRs, moves from soluble to membrane-bound compartments in a Ca^{2+}-dependent manner, and attenuates Ca^{2+} sparks. However, there were also notable differences between cardiac and smooth muscle sorcin that reveal exquisite adaptation of sorcin properties to its cellular environment. Part of this work has been published in abstract form (Rueda *et al.* 2005).

Methods

Antibodies

Polyclonal antisorcin antibody (Harlan Bioproducts for Science Inc., Indianapolis, IN, USA) was raised in rabbits against the C-terminus peptide of human sorcin. For Western blot and immunocytochemical analyses, additional primary antibodies against RyRs (monoclonal anti-RyR antibodies, clone C3-33 and clone 34C; Affinity BioReagents, Golden, CO, USA) and against phosphorylated RyR2 (rabbit anti-PS2809; Badrilla, UK) were used. Secondary peroxidase-conjugated antibodies were donkey anti-rabbit IgG (Amersham Biosciences, Piscataway, NJ, USA), goat anti-mouse, and goat anti-rabbit IgGs (Calbiochem, San Diego, CA, USA). Secondary fluorescence-labelled antibodies were Cy5 goat anti-rabbit (Jackson Immunolaboratories Inc. West Grove, PA, USA), Alexa Fluor 488 goat antirabbit IgGs and Alexa Fluor 568 goat antimouse IgGs (Molecular Probes, Eugene, OR, USA). Normal goat serum was from Vector Laboratories, Inc. (Burlingame, CA, USA).

Western blots for sorcin identification

Aorta, cerebral artery and heart homogenates were prepared with homogenization buffer (150 mM NaCl, 1% Igepal CA-630, 0.5% deoxycholate, 0.1% SDS, 2 mM EGTA, 50 mM Tris-HCl, pH 8.0) plus proteases inhibitors (μM: aprotinin, 0.52; benzamidine, 10; leupeptin, 12; PMSF, 100). Tissues were homogenized with a Brinkmann Polytron (three times for 30 s each at medium speed) and spun at 2000 *g* for 15 min. Supernatants were fractionated on 10% SDS-PAGE precast gels (Bio-Rad), transferred onto nitrocellulose membranes (1 h at 100 V, Hybond-ECL, Amersham Biosciences) and probed with anti-sorcin serum diluted 1 : 6000 in phosphate-buffered saline containing Tween-20 (PBS-T) buffer (3 mM KH_2PO_4, 10 mM Na_2HPO_4, 150 mM NaCl, 0.1% Tween 20, pH 7.2–7.4). Membranes were blocked for 2 h with 5% fat-free dry milk in PBS-T buffer before addition of the primary antibody. After washing 3 times with PBS-T buffer, membranes were incubated 1 h with secondary peroxidase-conjugated antibody (donkey anti-rabbit diluted 1 : 13 000 in PBS-T). Signal was detected by chemiluminiscence. When indicated, the relative amount of protein on the blots was determined by densitometry using LabWorks software (UVP Inc., Upland, CA, USA). Purified recombinant human sorcin, obtained as previously described (Farrell *et al.* 2003), was quantified spectrophotometrically at 280 nm using a molar extinction coefficient of 29 400 (Meyers *et al.* 1995*a*) and used as positive control in the blots. Protein concentration in all samples was assessed by the Bradford method.

Cerebral artery myocytes and cardiomyocytes isolation

Rat cerebral artery myocytes were enzymatically isolated from Sprague-Dawley rats (200–220 g). Rats were anaesthetized by peritoneal injection of pentobarbital solution (100 mg kg^{-1}) before decapitation in a protocol approved by the Animal Resource Center of the University of Wisconsin. The brain was removed and transferred to a Petri dish filled with ice-cold oxygenated dissociation solution (containing (mM): 55 NaCl, 6 KCl, 80 Na-glutamate, 5 $MgCl_2$, 10 glucose and 10 Hepes, pH 7.4). The cerebral basilar arteries were carefully dissected, cleaned of surrounding connective tissue and transferred to a 1.5 ml tube. The arteries were incubated for 40 min on ice in dissociation solution containing 1.5 mg ml^{-1} papain, 2 mg ml^{-1} BSA, and 1 mM dithiothreitol, followed by a 30 min incubation at 32°C in the same solution. Finally, the tissue was transferred to a collagenase solution (mixture of collagenase type F and type H, 7 : 3, Sigma Co.) and incubated for 15 min at 32°C with shaking. Enzyme digestion was stopped by washing the tissue 5 times with dissociation solution. Digested tissue was triturated with a fire-polished glass Pasteur pipette to yield single smooth muscle cells. Myocytes were kept at 4°C and used within the same day. Non-permeabilized myocytes were loaded with 10 μM Fluo-3 AM (Molecular Probes) for 40 min at room temperature. Then, cells were incubated in dissociation

solution containing 5 mM $CaCl_2$ to recover internal Ca^{2+} stores. Cells used for permeabilization procedures were not subjected to Fluo-3 AM loading. Ventricular cardiomyocytes used for immunostaining analysis were isolated as previously reported (Farrell *et al.* 2003).

Immunostainings of tissue sections and myocytes

Fresh aorta and basilar cerebral artery sections and cells were stained and imaged as reported before (Ohi *et al.* 2001; Eghbali *et al.* 2003; Farrell *et al.* 2003) with some modifications. Tissue sections (10 μm) and isolated myocytes were fixed by immersion in fixative (4% paraformaldehyde, 2% picric acid in 0.1 M PBS, pH 7.4), for 2 h (tissue sections) or 10 min (cells). Tissue and cells were permeabilized with 0.2% Triton X-100 in PBS for 1 h or 10 min, respectively. Non-specific binding was blocked with 5% normal goat serum (NGS) in PBS for 30 min. After washing, myocytes and tissue sections were incubated for 3 h at room temperature with anti-sorcin serum (1 : 3000 dilution in PBS containing 1% NGS) or preadsorbed antisorcin serum (control, with 300 μg ml^{-1} of purified recombinant sorcin), washed 5 times 5 min each with PBS containing Triton X-100 (0.2%), and incubated for 1 h with the indicated secondary antibody (Alexa Fluor-488- or Cy5-goat anti-rabbit, for single immunostainings). For double immunostainings of sorcin and RyRs, vascular and cardiac myocytes were subjected to an additional overnight incubation with primary RyR antibody (clone 34C) at 4°C, before sequential incubations (of 1 h each) with fluorescence secondary antibodies (Alexa Fluor 488-conjugated goat anti-rabbit, and Alexa Fluor 568-conjugated goat anti-mouse, respectively). Tissue sections or isolated cells were washed in PBS 3 times for 5 min each and mounted using Prolong (Molecular Probes). Control samples were stained in parallel, and confocal images were taken with the same laser intensity and microscope settings. Stacks of tissue images (Fig. 4) were acquired by optically sectioning tissues every 1 μm in the z-plane with an Olympus Fluoview confocal microscope by exciting Alexa Fluor 488 or Cy5 dyes at 488 or 633 nm with the argon and the red helium–neon line, respectively, and collecting fluorescence at 510 or above 660 nm, respectively. Cell images (Fig. 5) were acquired every 0.4 μm in the z-plane with a Zeiss LSM510 meta confocal microscope equipped with an ×63 oil-immersion objective (Zeiss plan-apochromat, N.A. 1.4) by alternating the excitation of Alexa Fluor 488 and 568 at 480 or 543 nm with the argon or helium–neon lines and collecting fluorescence at 505–530 or above 585 nm, respectively. The weighted colocalization coefficient (WCC) method of the Zeiss LSM 510 software (v. 3.2 SP2) was used to quantify the colocalization of sorcin with RyRs. This method weighs the intensity of pixels (brighter pixels contributing more than fainter pixels), according to the formula:

$$\mathrm{WCC} = \frac{\sum i\mathrm{Pi,\ coloc}}{\sum i\mathrm{Pi,\ total}}$$

where Pi,coloc is the intensity of colocalizing pixels and Pi, total is the intensity of any non-zero value pixels. The cross-hair markers in the scattergrams were positioned above the mean pixel intensity +2 standard deviations for each Alexa channel. WCC value range from 0 to 100, where 0 represents no colocalization and 100 means all pixels colocalize.

Ca^{2+}-dependent translocation of endogenous sorcin

To examine whether endogenous sorcin was able to translocate from cytosol to membranous compartments in vascular tissue, dog aorta tissue was cleaned of endothelial and serosa layers and the remaining tissue (mostly smooth muscle layers) was homogenized with a Brinkmann Polytron (3 times × 30 s at medium speed) in saline solution (0.9% NaCl, 10 mM Tris-HCl, 2 mM EGTA, pH 7.2) plus the protease inhibitors described above. Homogenates were then diluted to ∼3 mg ml^{-1} in the same solution plus 2 mM EGTA and $CaCl_2$ necessary to set free [Ca^{2+}] to 0 (< 50 nM), 0.1, 1, 10, 100 and 1000 μM (with affinity constants given in WinMAXC 2.5, Chris Patton, Stanford University) and incubated for 10 min at 37°C. The incubation was terminated by centrifugation at room temperature for 40 min at 100 000 g. Equal protein amounts of supernatant and pellets were analysed by Western blots using sorcin antibody as described above. The relative amount of sorcin on the blots was determined by densitometry using LabWorks Software.

Immunoprecipitation studies

Homogenates of aorta and heart tissues were prepared with homogenization buffer plus protease inhibitors as describe above. Aliquots of 1 ml with ∼12 mg of protein were precleared with 20 μl of protein A–Sepharose beads (Amersham Biosciences) before incubation with 2.5 μl of either anti-sorcin or control serum (preimmune serum from the same rabbit) for 2 h at 4°C in the rocker device, without or with 10 μM $CaCl_2$. Protein A–Sepharose beads (20 μl) were then added to the medium and incubation continued for 2 h at 4°C. Beads were washed 4 times for 5 min each, with 1 ml of homogenization buffer. The protein complexes were eluted with Laemmli sample buffer (250 mM Tris-HCl, 400 mM dithiothreitol, 8% SDS, 0.04% bromphenol blue, 50% glycerol, pH 6.8), and assayed for sorcin (see above) and RyR2 by Western blot analysis. For detection of RyR2, proteins were subjected to 4 h SDS-PAGE, at 100 V and then transferred

onto nitrocellulose membranes (2 h, 100 V at 4°C). Membranes were blocked overnight with 5% fat-free milk, incubated with monoclonal anti-RyR2 antibody (1 : 2000 dilution in PBST, clone C3-33) or anti-PS2809 antibody (1 : 2500 dilution in PBST), for 3 h at room temperature in the rotating device. After 3 washes of 10 min each, the corresponding secondary antibody was added, and incubated for an additional hour. Detection was by chemiluminiscence.

Permeabilization procedure and Ca^{2+} sparks recordings

Saponin permeabilization of rat VSMCs was conducted as described by Lukyanenko & Györke, 1999) for cardiac myocytes, with some additional modifications. Isolated myocytes (50 μl of cell suspension) were allowed to adhere to the bottom of a glass coverslip in a perfusion chamber (P6, Warner Instruments, Hamden, CT, USA). Fluo-3 loaded myocytes were perfused with hepes-buffered saline solution (HBSS) solution (mM: 137 NaCl, 5 KCl, 4 $NaHCO_3$, 2 $MgCl_2$, 2 $CaCl_2$, 0.42 KH_2PO_4, 10 glucose and 10 Hepes, pH 7.4) to record Ca^{2+} sparks in control condition (intact cells). When recording Ca^{2+} sparks in permeabilized cells, myocytes were perfused for 1 min with dissociation solution supplemented with EGTA (0.5 mM) before permeabilization. Cells were permeabilized with saponin (0.005% for 60–90 s) in permeabilization solution containing (mM): 110 Na-aspartate, 30 NaCl, 6 KCl, 0.5 EGTA, 8% dextran, 20 Hepes, and 0.05 Fluo-3 pentapotassium salt (Molecular Probes), pH 7.2. When permeabilization was complete (monitored by the appearance of fluo-3 signal into the cytosol), cells were equilibrated for 1 min in internal solution (mM: 110 K-aspartate, 10 NaCl, 30 KCl, 3 MgATP (free $[Mg^{2+}]$ adjusted to ~1 mM), 10 phosphocreatine, 0.05 Fluo-3 pentapotassium salt, 5 units ml^{-1} creatine kinase, 8% dextran, pH 7.2), with low (0.02 mM) or high concentration of EGTA (0.5 mM). Appropriate amounts of $CaCl_2$ were added to have a free $[Ca^{2+}]$ of 100 nM. The free $[Ca^{2+}]$ was calculated with WinMAXC 2.5 (Chris Patton, Stanford University) and verified by measurements with a fluorescence spectrofluorometer (Hitachi F-4500) and the calcium indicator Fura-2. All solutions were applied onto the cells with a microperfusion system with a three-barrelled pipette (Warner Instruments), and recordings were done at room temperature. Spontaneous Ca^{2+} release events were recorded in internal solutions (with low or high [EGTA]) in the presence or the absence of sorcin (2 μM) with a laser scanning confocal microscope (Zeiss, LSM510 META) equipped with a ×63 oil-immersion objective (N.A. 1.4) in the line scan mode. The scan line was orientated along the long axis of the myocytes at a speed of 1.92 ms per line. Fluo-3 was excited at 488 nm with an argon laser (3% intensity), with emitted fluorescence measured at above 510 nm. Ca^{2+} sparks were reconstructed by stacking consecutive 4 s line scans and performing a time–intensity plot. Ca^{2+} sparks were automatically detected and measured with a custom-made program running in IDL 5.5 software (ITT Visual Information Solutions, Boulder, CO, USA), with a detection threshold of 4.3 × s.d. Images were normalized by dividing the fluorescence intensity of each pixel (F) by the average resting fluorescence intensity (F_0) of a confocal image to generate an F/F_0 image.

Statistical data analysis

Data are expressed as means ± s.e.m. The number of cells or Ca^{2+} sparks is specified in the text. Statistical significance of the changes in spark characteristics was assessed by Student's t test or by one-way ANOVA with either Student-Newman-Keuls, or non-parametric Dunn's tests, wherever applicable, using SigmaStat 3.0 software (Systat Software Inc., Point Richmond, CA, USA). Values of $P < 0.05$ were considered significant.

Results

Sorcin expression in heart, aorta and cerebral artery tissues

Western blots of heart, aorta and cerebral artery rat homogenates (30 μg of protein per well) probed with sorcin antibody revealed a single discrete band (Fig. 1*A*, lane 2–4) of relative mobility comparable to purified recombinant sorcin (Fig. 1*A*, lane 5). The molecular weight (assessed by migration distance, R_f) for sorcin in SDS-PAGE was calculated with molecular weight standards (Bio-Rad) using LabWorks software. Heart and smooth muscle sorcin show a molecular weight of ~19.5 kDa, which is in agreement with previous reports (Meyers *et al.* 1985, 1987) and differs slightly from the molecular weight calculated by mass spectrometry (21.6 kDa). Sorcin antibody specificity was demonstrated by preadsorbing the immune serum with purified recombinant sorcin. Sorcin expression in heart homogenates has been reported before (Meyers *et al.* 1995*b*; Lokuta *et al.* 1997; Farrell *et al.* 2003) and we used it here as an index of relative density to assess sorcin expression in vascular tissue. Western blot analysis showed that the expression of sorcin in rat aorta was ~2-fold higher than that found in heart (1.91 ± 0.1 *versus* 1.00 ± 0.1 normalized optical density $n = 3$; Fig. 1*C*), and in cerebral artery (0.85 ± 0.1 normalized optical density). Therefore, sorcin appears to be more abundant in aorta than in heart and cerebral arteries, perhaps reflecting a more prominent role in this tissue.

Sorcin localization in endothelial and smooth muscle cells of aorta and cerebral arteries

Immunofluorescence labelling of transverse sections of aorta (Fig. 2*A*) and cerebral artery (Fig. 2*B*) with anti-sorcin serum revealed high levels of sorcin expression in endothelial and subendothelial smooth muscle cells (see arrows). Confocal images at higher magnification (×60, right panels) showed strong fluorescent signal throughout the cytoplasm but not within the nuclei in smooth muscle cells. As can be appreciated in Fig. 2*A*, the elastic lamellae in the medium are not stained. Also, the endothelial cells of the small artery in the aorta section are strongly positive for sorcin antibody. Control tissue sections labelled with preadsorbed serum (with purified recombinant sorcin, 300 $\mu g\,ml^{-1}$) but exposed to secondary antibody and imaged under identical conditions revealed no intracellular fluorescence (labelled 'Ab + Ag').

Ca^{2+} dependence of endogenous sorcin translocation

Quantitative Western blotting of aortic subcellular fractions shows that the relative density of sorcin is 3.7-fold higher in microsomal particulates than in whole homogenates (0.22 ± 0.05 *versus* 0.06 ± 0.03 ng sorcin per μg of protein loaded in the gel, $n = 5$; not shown), suggesting that smooth muscle sorcin, like cardiac muscle sorcin (Farrell *et al.* 2003), translocates from soluble to membranous compartments to interact with target proteins. Cardiac sorcin translocation is Ca^{2+} dependent (Farrell *et al.* 2003; Matsumoto *et al.* 2005); we thus tested whether smooth muscle sorcin was able to translocate from cytosolic to membranous compartments depending on free $[Ca^{2+}]$. Figure 3 shows that smooth muscle sorcin gradually associates with microsomal fractions in a Ca^{2+}-dependent manner. Aorta homogenates were incubated in medium containing the free $[Ca^{2+}]$ indicated in Fig. 3*A* and *B* and then centrifuged at high speed to separate soluble from membranous components. At 0 μM $[Ca^{2+}]$ (~4 nM, calculated free $[Ca^{2+}]$), the vast majority of sorcin is found in the supernatant (Fig. 3*A*); conversely, only traces of sorcin are found in the membranous component (pellet, Fig. 3*B*). This relationship is gradually inverted with increasing $[Ca^{2+}]$ so that at 1000 μM $[Ca^{2+}]$, the highest concentration tested, only ~20% of sorcin is soluble. The Ca^{2+} dependence of sorcin translocation was sigmoidal and could be fitted with a Hill equation that yields a half-maximal effective $[Ca^{2+}]$ (EC_{50}) of 1.5 ± 0.4 μM ($n = 3$) and cooperativity coefficient (n_H) of 1.4 ± 0.2 (Fig. 3*C*). The EC_{50} is close to previous estimations of the sorcin–Ca^{2+} high affinity site (~1 μM, Zamparelli *et al.* 1997; Mella *et al.* 2003) determined *in vitro* but differs substantially from the EC_{50} for Ca^{2+}-dependent translocation of sorcin in cardiac cells (~200 μM, Farrell *et al.* 2003). None of these EC_{50} values, however, is similar to the EC_{50} needed for Ca^{2+}-dependent *precipitation* of sorcin (incapacity to remain soluble in the absence of membrane-embedded targets). Figure 3*C*, open circles, shows normalized sorcin absorbance ($A_{280\,nm}$)

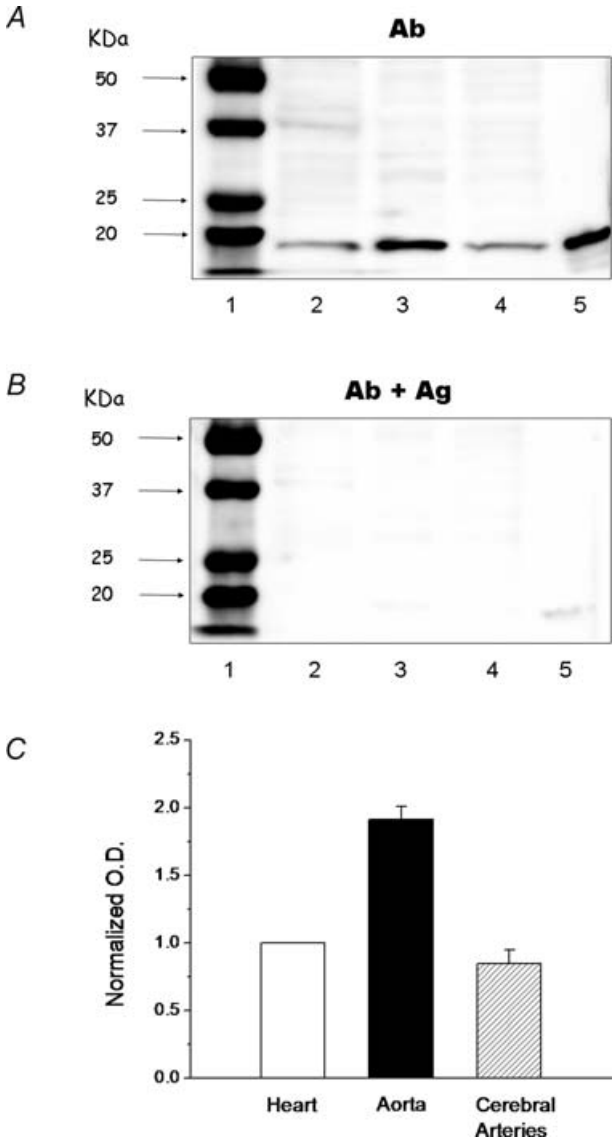

Figure 1. Sorcin expression in cardiac and vascular tissues
Western blot of rat tissue homogenates probed with sorcin antibody. *A*, samples containing 30 μg of protein from whole homogenates of heart (lane 2), aorta (lane 3) and cerebral arteries (lane 4) or 30 ng of purified recombinant sorcin (lane 5, positive control) were run on 10% acrylamide gels, blotted onto nitrocellulose membranes and probed with sorcin antibody (1 : 6000). Smooth muscle sorcin was detected at the same position as purified sorcin. *B*, Western blot done as in *A* except that the sorcin antibody was preadsorbed with 300 μg of purified sorcin for 30 min before incubation with the proteins. The secondary antibody was peroxidase-conjugated donkey anti-rabbit and detection was by chemiluminiscence. Lane 1 contains molecular weight standards detected with Precision Streptactin-HRP conjugate (Bio-Rad). *C*, bar graph showing the relative amount of sorcin on the blots ($n = 3$) determined by densitometry using LabWorks software. Signal intensity was normalized with respect to heart levels.

versus $[Ca^{2+}]$ in the absence of membrane proteins. The curve shows biphasic decay. The steepest decrease in absorbance (83%) may be fitted with a sigmoidal function with an $EC_{50} = 750\ \mu M$. This absorbance reduction most likely reflects sorcin precipitation due to exposure of hydrophobic domains induced by Ca^{2+} binding. A much smaller drop in absorbance appears at very low $[Ca^{2+}]$ ($EC_{50} = 200$ nM) and probably reflects dimerization of sorcin (with concomitant shift in absorbance) or other conformational changes. In neither case, however, are these changes comparable to those observed when sorcin is exposed to similar $[Ca^{2+}]$ *in the presence* of aorta homogenates (this study, $EC_{50} = 1.5\ \mu M$) or permeabilized cardiomyocytes (Farrell *et al.* 2003, $EC_{50} \approx 200\ \mu M$), clearly indicating that they correspond to different phenomena.

Endogenous smooth muscle sorcin associates with RyRs

Sorcin interaction with cardiac RyRs (RyR2) has been well documented (Meyer *et al.* 1995; Lokuta *et al.* 1997; Farrell *et al.* 2003) and RyR2 appears to be a major RyR isoform in vascular smooth muscle cells (Herrmann-Frank *et al.* 1991; Gollasch *et al.* 1998; Yang *et al.* 2005). We thus tested whether endogenous sorcin was able to interact with RyR2 in aortic tissue (Fig. 4). As a positive control, we used cardiac homogenates, which only express RyR2 isoforms. Western blots first showed the ability of sorcin antibody to effectively immunoprecipitate endogenous sorcin from solubilized aortic and cardiac homogenates (Fig. 4*A*). Immunoprecipitation of sorcin was enhanced by Ca^{2+} in aortic and cardiac homogenates,

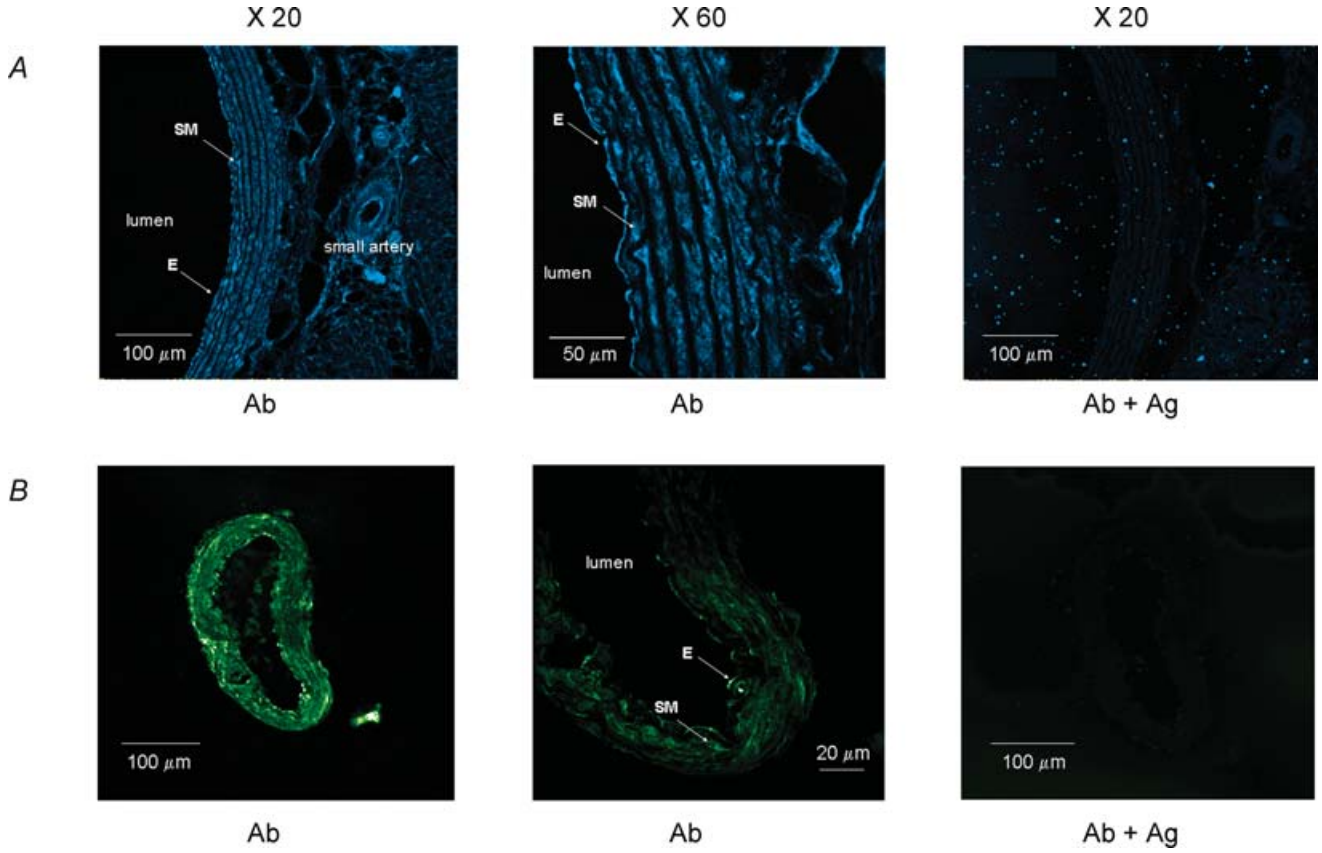

Figure 2. Sorcin immunostainings of aorta and cerebral artery tissue sections
A, aorta transverse sections (10 μm) were immunostained using sorcin antibody (Ab) and detected with Cy-5 goat anti-rabbit IgG. *B*, basilar cerebral artery transverse sections (10 μm) were also immunostained using sorcin antibody (Ab) and detection was with Alexa Fluor 488-goat anti-rabbit IgGs. Arrows indicate specific immunostaining seen throughout the cytoplasm in endothelial (E) and smooth muscle (SM) cells. No fluorescence signal was detected when the sorcin antibody was preadsorbed with 300 $\mu g\ ml^{-1}$ of purified recombinant sorcin before being incubated with the tissue (Ab + Ag).

albeit the Ca^{2+} dependence was less pronounced in heart (Fig. 4*A*). We then tested whether RyR2 was present in the immunoprecipitation complexes. Screening of these sorcin immunoprecipitates with RyR2 antibody confirms the presence of a RyR2 band in heart and reveals the presence of a similar band in aortic immunoprecipitates (Fig. 4*B*). RyR2 isoform specificity was demonstrated with the RyR2-(PO4)-S2809 antibody (Fig. 4*C*), which is directed against the phosphorylated epitope ^{2802}YNRTRRIS(PO4)QTS2812 of RyR2, not present in RyR1 or RyR3 (Rodriguez *et al.* 2003). Cardiac RyR immunoprecipitations appear to be more Ca^{2+} dependent; however, they all appear specific, as the use of preimmune sorcin serum from the same rabbit yields no bands (labelled 'Control Ab').

Sorcin and RyRs colocalize in isolated myocytes

To determine the precise intracellular localization of sorcin and whether it interacts with RyRs within the same myocyte, freshly isolated cerebral artery cells and ventricular cardiomyocytes were labelled with antisorcin serum in combination with RyR antibodies. Images from these double-labelling experiments are presented in Fig. 5. Confocal images of a cerebral artery myocyte (0.7 μm thick) show a disperse distribution of sorcin in the cytosol combined with increased sorcin fluorescence signal at regions underneath the plasmatic membrane (Fig. 5*Aa*). The RyR spot-like distribution is more restricted and follows mainly the peripheral regions that are in close apposition to the plasmatic membrane (Fig. 5*Ab*). In the merged image (Fig. 5*Ac*) the orange/yellow labelling indicates sorcin–RyR overlap, which is only apparent in the SR regions close to the plasmatic membrane or junctional gaps. By contrast, sorcin and RyR2 distributions in cardiac cells run specifically on top of the cross-sectional striations of the cell (Fig. 5*B*). Within each transverse band in the merged image (Fig. 5*Bc*), sorcin and RyR fluorescence intensify at discrete spots, suggesting that the proteins are organized in clusters rather than being uniformly distributed.

The colocalization images of Fig. 6*Aa* and *Ba* display only the pixels that include sorcin and RyR labelling from the merged images of Fig. 5. The crosshair thresholds for identification of positive structures in the scattergram was set above the mean pixel intensity + 2 standard deviations for each Alexa derivative and represented at least ~23% of the total fluorescence, thus ensuring that only the pixels with significantly strong fluorescence overlap were displayed. On an intensity scale of 0–4095, the RyR and sorcin channels threshold was 944 and 938 for vascular (Fig. 6*Ab*) and 1741 and 1050 for ventricular (Fig. 6*Bb*) myocytes, respectively (i.e. region 3 of their respective scattergrams). Figure 6*Aa* shows that the punctuate pattern seen in vascular myocytes is prevalent at regions close to the plasmatic membrane and where the SR is found. Using the automated weighted colocalization coefficients method (see Methods) to set the colocalization threshold, typically ~57% of pixels labelled with sorcin colocalized with ~61% of RyR-labelled pixels (Fig. 6*Ab*); the remaining sorcin was predominantly cytosolic, where few RyR-labelled pixels were found. When the colocalization threshold was higher, such as that shown in the scattergram of ventricular cardiomyocytes ($\geq$ 42% of total fluorescence), only ~30% of sorcin pixels colocalize with 34% of RyR-labelled pixels (not shown). These results contrast with those obtained with ventricular myocytes (Fig. 6*Ca*), where a

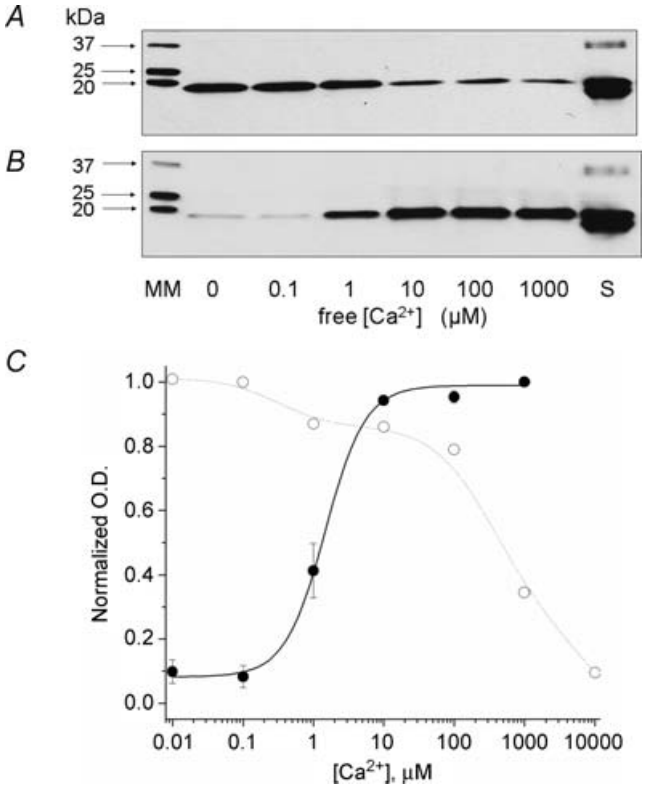

Figure 3. Ca^{2+}-dependent translocation of sorcin in smooth muscle tissue
Western blots of aortic supernatants (*A*) and corresponding pellets (*B*) with sorcin antibody. Whole dog aorta homogenates were incubated with specified free [Ca^{2+}] for 10 min at 37°C (pH = 7.2) and centrifuged at room temperature, for 40 min at 100 000 *g* to separate sorcin from cytosolic and membranous compartments. Proteins in supernatant and pellet fractions were separated by gel electrophoresis (20 μg per well), transferred to a nitrocellulose membrane and probed with the sorcin antibody. Smooth muscle sorcin was detected in the same position as purified recombinant sorcin (S). *C*, sorcin bands in *B* were normalized with respect to the sorcin band signal at free [Ca^{2+}] = 1000 μM and the data are plotted as filled circles. Continuous line is a Hill equation fitting of these data with EC_{50} = 1.5 μM and n = 1.4 (n = 3). Open circles are normalized O.D. (A280) nm readings of a solution containing 1 μM sorcin, 1 mM EGTA, various $CaCl_2$ that yield the specified free [Ca^{2+}]. Membrane fractions were omitted.

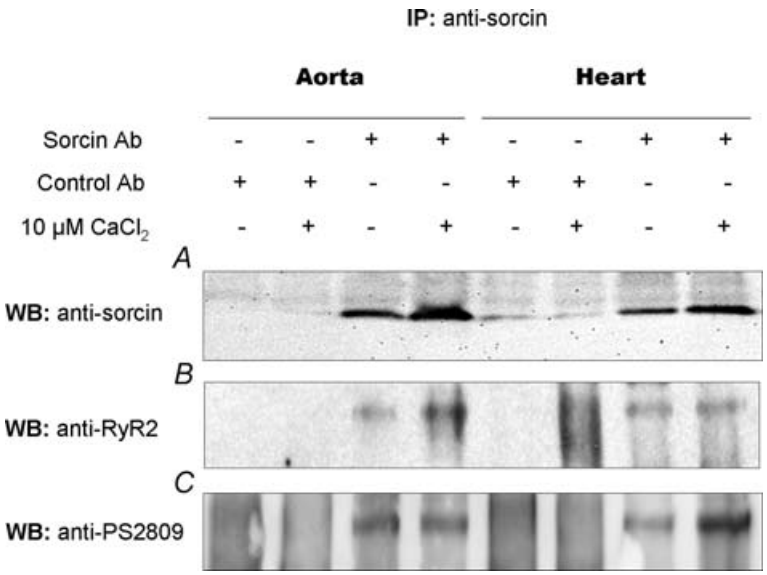

Figure 4. Sorcin antibody coimmunoprecipitates smooth muscle RyR2
Western blots of dog aorta proteins immunoprecipitated with sorcin antibody. Aliquots of homogenate containing 12 mg of protein per ml were incubated for 1 h at room temperature with 1 : 400 dilution of either sorcin antibody or control serum (preimmune serum from the same rabbit), with or without Ca^{2+} (10 μM). Antibody–antigen complexes were precipitated with immobilized protein A–sepharose. Antigens were solubilized in Laemmli buffer for 5 min before examination by gel electrophoresis.

pool of sorcin closely follows the orderly pattern of RyR2 distribution, brilliantly decorating the transverse tubules at regularly spaced intervals of ~1.7 μm (Fig. 6*Cb*), i.e. the mean sarcomere length in a fixed cardiac myocyte (Powell *et al.* 2004). The scattergram of Fig. 6*Bb* shows that this pool of RyR2-colocalized sorcin pixels comprises ~47% of total sorcin pixels. The remaining sorcin staining appears mostly in patches underneath the sarcolemma (Fig. 6*Ba*). Hence, our examination of VSM cells suggests that a small but significant fraction of sorcin, predominantly that of peripheral location, colocalizes with a pool of RyRs comprising less than half of the total population.

Sorcin attenuates the amplitude, duration and spatial spread of spontaneous Ca^{2+} sparks in permeabilized smooth muscle cells. Ca^{2+} sparks in cerebral artery myocytes are, like in cardiac cells, localized and brief Ca^{2+} release events caused by the coordinated activity of clusters of RyRs (Nelson *et al.* 1995; Jaggar *et al.* 1998, 2000; Gollasch *et al.* 2000). Like in the heart, too, RyR2 in vascular smooth muscle appears to be the major RyR isoform involved in the generation of Ca^{2+} sparks (Gollasch *et al.* 2000; Ji *et al.* 2004), but there is no evidence yet that endogenous sorcin regulates Ca^{2+} spark activity in this tissue. We thus examined the spatio-temporal characteristics of spontaneous Ca^{2+} sparks in freshly isolated intact and permeabilized cerebral artery myocytes in the absence and presence of purified recombinant sorcin. Spontaneous Ca^{2+} sparks were recorded in Fluo3-loaded cells with a confocal microscope in line-scan mode. In the intact, non-permeabilized condition, Ca^{2+} sparks were observed with a frequency of 0.010 ± 0.001 events s^{-1} μm^{-1} and amplitude of 1.75 ± 0.04 F/F_0 (27 cells, 151 sparks, Fig. 7*A*, Table 1). The duration (measured as full duration

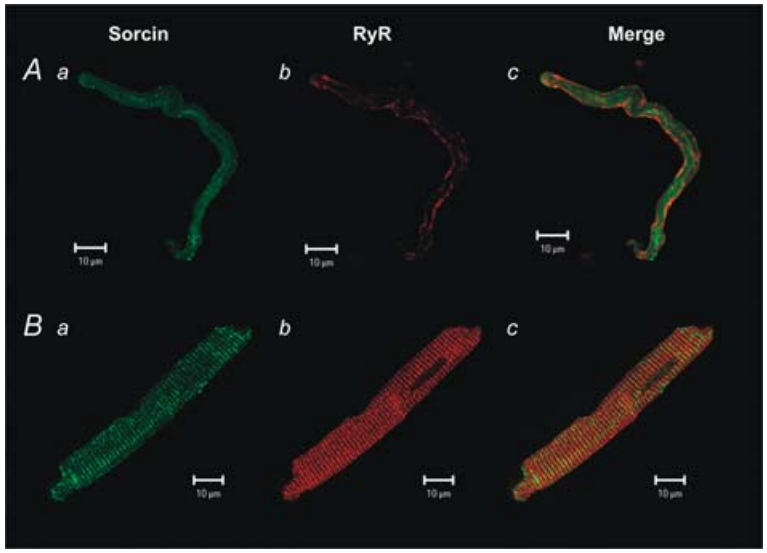

Figure 5. Double immunostaining of sorcin and RyRs in cerebral artery myocytes and cardiac cells
Confocal images of sorcin (*a*) and RyR (*b*) distribution in a cerebral artery smooth muscle cell (*A*) and in a ventricular cardiomyocyte (*B*). Sorcin antibody was detected with Alexa Fluor 488-goat anti-rabbit antibody (*a*), whereas RyR antibody (clone 34C) was detected with Alexa Fluor 568 goat anti-mouse antibody (*b*). Images (0.7 μm thick in the *z*-plane) were acquired simultaneously with a confocal microscope (Zeiss LSM510 META). All pixels are superimposed in the merged images (*c*) and overlapping is coded orange/yellow.

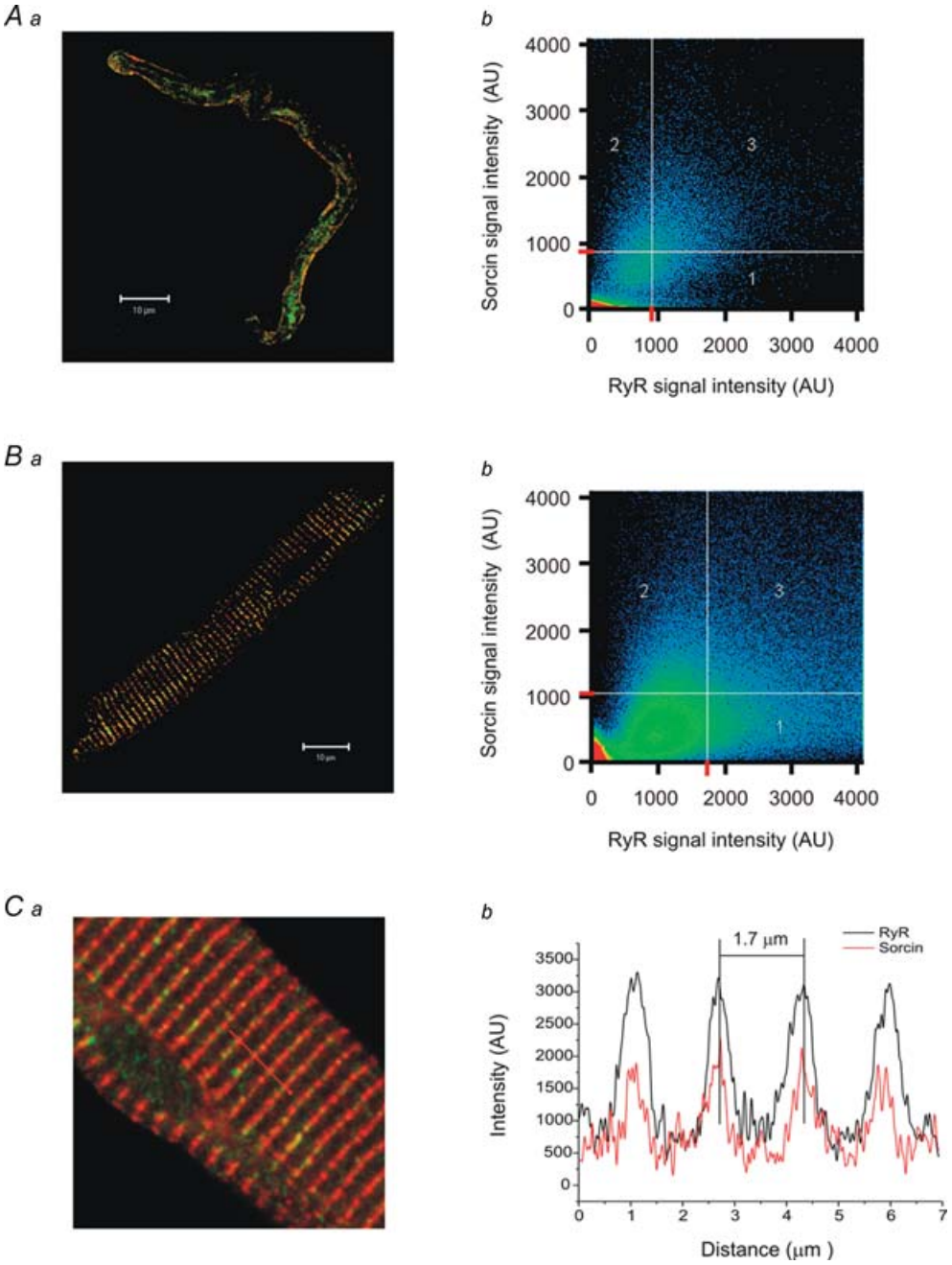

Figure 6. Sorcin-RyR colocalization analysis
A, sorcin and RyR colocalized pixels from the cerebral artery myocyte in Fig. 5 were extracted and superimposed in *a*; they correspond to region 3 of the scattergram (*b*). Same procedure was applied to the ventricular myocytes in *B*. Scattergrams show the pixel intensity distribution for the fluorescence of each Alexa Fluor (488 and 568). The crosshair lines in the scattergrams were positioned above the calculated background threshold for each Alexa. The crosshair lines define four regions: region 1 corresponds to RyR pixels only; region 2 corresponds to sorcin pixels only; region 3 contains the pixels where the sorcin–RyR overlap is the greatest; region 4 corresponds to sub-thoeshold pixels. Co-localization analysis was performed with Carl Zeiss LSM 5 software (version 3.2, SP2). *Ca*, image of a cardiomyocyte to show the fluorescence intensity distribution of sorcin and RyRs across several T-tubules (red line). *Cb*, intensity–distance plot showing sorcin (red) and RyR (black) fluorescence intensity peaks. The distance between T-tubules was ~1.7 μm.

at half-maximum amplitude) and size (measured as full width at half-maximum amplitude) of Ca^{2+} sparks were 55.5 ± 2.6 ms and 2.6 ± 0.1 μm, respectively, values which are close to those of Ca^{2+} sparks of adult rat cerebral artery myocytes (Gollasch *et al.* 2000). The addition of a submaximal concentration of caffeine (0.5 mM) into the recording chamber increased Ca^{2+} spark frequency 1.5-fold (0.015 ± 0.007 events s^{-1} μm^{-1}, $n = 23$ sparks), amplitude 1.3-fold ($F/F_0 = 2.26 \pm 0.12$), duration ~2-fold (FDHM = 115.3 ± 12.6 ms) and spatial spread 1.4-fold (FWHM = 3.6 ± 0.3 μm), indicating that these were *bona fide* RyR-originated Ca^{2+} sparks.

Permeabilization of external membranes was achieved by perfusion of a solution containing 0.005% saponin, 0.5 mM EGTA, and 50 μM Fluo-3 (salt) for ~60–90 s. Once the cell membrane was permeable (monitored

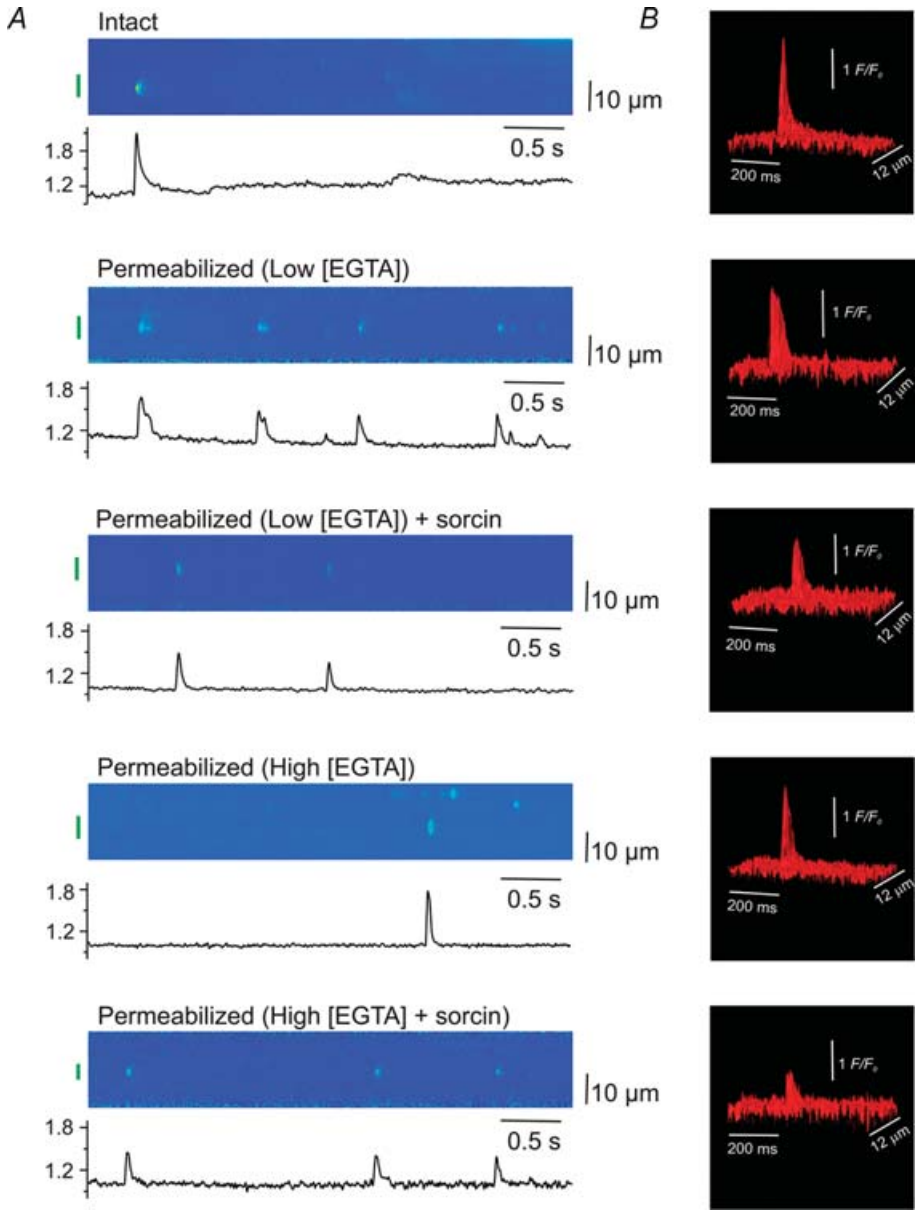

Figure 7. Spatio-temporal properties of Ca^{2+} sparks in intact and permeabilized rat cerebral artery myocytes

A, normalized representative line scan images (acquired at 1.92 ms $line^{-1}$) and corresponding intensity plots (below the images) of one release site per image (green bar) that show the spontaneous local Ca^{2+} events observed in Fluo-3 loaded intact or permeabilized myocytes under the specified conditions. The scan line was orientated in parallel with the long axis of the cell. The fluorescence intensity was normalized to the resting fluorescence intensity within the same cell. *B*, surface plot of a representative Ca^{2+} spark from the corresponding line scan indicating measures used for spark characteristics.

Table 1. Spatio-temporal properties of Ca^{2+} sparks in intact and permeabilized cerebral artery myocytes under different conditions

Treatment	Frequency (events s^{-1} μm^{-1})	Amplitude (F/F_0)	Duration (ms)	Width (μm)
Intact (151)	0.010 ± 0.001	1.75 ± 0.04	55.5 ± 2.6	2.6 ± 0.1
Permeabilized				
Low [EGTA] (61)	0.024 ± 0.004*	1.47 ± 0.02*	84.0 ± 7.6 *	2.9 ± 0.2
Low [EGTA] + sorcin (36)	0.020 ± 0.006*	1.32 ± 0.02*†	45.1 ± 4.4*†	2.3 ± 0.2†
Low [EGTA] + F112L-sorcin (144)	0.025 ± 0.003*†	1.49 ± 0.01*†	58.2 ± 3.2*†	2.94 ± 0.1†
Permeabilized				
High [EGTA] (123)	0.019 ± 0.003*	1.71 ± 0.04	42.3 ± 2.2*	2.2 ± 0.08 *
High [EGTA] + sorcin (62)	0.017 ± 0.004*	1.46 ± 0.03*†	34.7 ± 2.0 *†	1.95 ± 0.11 *†

Data presented as mean ± S.E.M. of measurements. Number of Ca^{2+} sparks recorded is indicated in parenthesis. *Significant difference ($P < 0.05$) with intact Ca^{2+} spark parameters. †Significant difference ($P < 0.05$) with parameters in the row above, for example, the frequency of Ca^{2+} sparks in cells perfused with F112L-sorcin was significantly higher than that in cells perfused with WT-sorcin. Duration and width were measured at half-maximal amplitude.

by the presence of membrane-impermeant Fluo-3 into the cytosol), an internal solution with low (0.02 mM) or high (0.5 mM) [EGTA] was introduced and Ca^{2+} sparks were recorded after 2 min of equilibration (see Methods). Under low Ca^{2+} buffering conditions (low [EGTA]), Ca^{2+} sparks were observed with an increased frequency (0.024 ± 0.004 events s^{-1} μm^{-1}; 6 cells, 61 sparks; Fig. 7*A* and Table 1), duration (84.0 ± 7.6 ms) and spatial spread (2.9 ± 0.2 μm), but decreased amplitude (1.47 ± 0.02 F/F_0) with respect to intact cell data. Thus, permeabilization modifies significantly the characteristics of Ca^{2+} sparks in patterns that appear unpredictable, but the increase of spark frequency in permeabilized cells suggests that the internal solution used to mimic the cytosolic milieu lacks components that appear to restrain RyR activity in intact cells.

To test the hypothesis that sorcin dissociation and washing from permeabilized cells may be responsible, at least in part, for the changes in Ca^{2+} spark properties observed upon permeabilization, we recorded Ca^{2+} sparks after equilibration (2 min perfusion) of permeabilized myocytes with 2 μM recombinant purified sorcin. While the physiological concentration of sorcin in cerebral artery myocytes has not been determined, it appears to be close to 1 μM in cardiac cells (Meyers *et al.* 1995*b*), thus providing a good estimate of the concentration of sorcin to be tested here. Table 1 and Fig. 7 show that 2 μM sorcin decreases the duration of Ca^{2+} sparks to levels comparable to those seen in intact cells (45.1 ± 4.4 ms, $n = 6$ cells, 36 sparks). However, sorcin exaggerated the reduction in Ca^{2+} spark amplitude (1.32 ± 0.02 F/F_0) and spatial spread (2.3 ± 0.2 μm) seen upon permeabilization. Thus, direct perfusion of sorcin onto weakly buffered permeabilized cells restores some, but not all the Ca^{2+} spark parameters affected by permeabilization. These effects of sorcin appear to be dependent on its ability to interact with RyR2 more than on its bulk structure or electrical charge inasmuch as F112L-sorcin, a single-amino acid mutant that lacks the potency of wild-type sorcin to modulate RyR2 activity (Mohiddin S, Antaramian A, Gómez AM, Farrell EF & Lin J-P 2005, unpublished observations) had limited effect on Ca^{2+} sparks properties. Table 1 shows that, except for Ca^{2+} spark duration, all other parameters in cells perfused with F112L-sorcin were significantly different from those obtained in the presence of WT-sorcin; by contrast, they closely resembled those obtained *in the absence of sorcin* (Table 1).

We next increased the Ca^{2+} buffering capacity of the internal solution (with 0.5 mM EGTA) without modifying free [Ca^{2+}] and determined Ca^{2+} spark properties in the absence and presence of sorcin. The increase in Ca^{2+} buffering capacity alone resulted in decreased duration (42.3 ± 2.2 ms, 14 cells, 123 events, Table 1) and size (2.2 ± 0.1 μm, 14 cells) of Ca^{2+} sparks with respect to intact cells, as expected. The frequency was again higher than that in intact cells (0.019 ± 0.003 events s^{-1} μm^{-1}), but lower than that obtained in low Ca^{2+} buffering strength (Table 1), also as expected. Remarkably, addition of 2 μM sorcin decreased even more the amplitude (1.46 ± 0.03 F/F_0, 10 cells, $n = 62$ events), duration (34.7 ± 2.0 ms), and spatial spread (1.95 ± 0.11 μm) of Ca^{2+} sparks without producing notable effects on Ca^{2+} spark frequency (0.017 ± 0.004 events s^{-1} μm^{-1}). Thus, sorcin can substantially modify the behaviour of RyRs in permeabilized cells without substantially modifying Ca^{2+} spark frequency; rather, it appears to alter the time that RyRs remain open. This notion is supported by the fact that sorcin significantly decreases the amplitude and duration of Ca^{2+} sparks, especially when low Ca^{2+} buffering conditions were used but also when Ca^{2+} buffering was stronger.

Discussion

This study reports for the first time the expression, intracellular location and Ca^{2+}-dependent translocation

of sorcin in smooth muscle (cells and tissue sections) while getting some insight into its physiological role as modulator of Ca^{2+} sparks in this tissue. Sorcin was present in both endothelium and smooth muscle from aorta and cerebral arteries (Fig. 2), tissues that express RyRs at lower density than cardiac cells (Hermann-Frank *et al.* 1991; Gollasch *et al.* 1998); yet, sorcin expression in vascular smooth muscle was similar or higher than that in ventricular cardiomyocytes (Fig. 1). If we assume that RyRs are one of sorcin's major target proteins (Meyers *et al.* 1995*b*; Lokuta *et al.* 1997; Farrell *et al.* 2003), the latter suggests that sorcin may have a prominent role in regulating RyR activity in VSM. Our immunoprecipitation studies (Fig. 4) provided evidence to postulate that smooth muscle RyRs are indeed sorcin's molecular partners and revealed also a potential function for sorcin in this tissue. The direct recording of Ca^{2+} sparks in the absence and presence of sorcin (Fig. 7) confirmed a role for this protein in regulating RyR activity.

We found that, like in the heart, endogenous sorcin of smooth muscle cells moves between soluble, cytosolic compartments and membrane-embedded targets as a function of $[Ca^{2+}]$ (Fig. 3). However, unlike in the heart, where this process requires an apparently physiologically unattainable intracellular $[Ca^{2+}]$ ($EC_{50} \approx 200\ \mu M$, Farrell *et al.* 2003), Ca^{2+}-dependent translocation of sorcin in smooth muscle is achieved at Ca^{2+} levels compatible with those measured during the peak of contraction ($EC_{50} = 1.5\ \mu M$). This difference is congruent with our hypothetical role for sorcin. In our scheme, sorcin translocation in *cardiac cells* would be promoted only in the dyadic space (the gap between T-tubules and SR membranes), where the tight interaction between VDCC and RyR2 generates Ca^{2+} gradients that have been estimated to reach several hundred micromolar (Peskoff & Langer, 1998). In *smooth muscle cells*, on the other hand, the concept of 'loose coupling' (Collier *et al.* 2000; Kotlikoff, 2003) has gained ground as it becomes evident that VDCC and RyRs do not share privileged venues of communication. Then, the Ca^{2+} gradients formed at the peripheral release sites in smooth muscle cells would be, albeit small and quickly dissipating, adequate for sorcin translocation. Nonetheless, the difference in Ca^{2+}-dependent translocation spans more than two orders of magnitude and is surprising given that sorcin is structurally identical in all tissues (one unique *sorcin* gene) and even more if we assume that at least one of sorcin's major interacting partners (RyR2) appears to be structurally identical in cardiac and smooth myocytes (Hermann-Frank *et al.* 1991; Yang *et al.* 2005). Although elucidation of this difference will require further studies, we favour the notion that the enormous difference in $[Ca^{2+}]$ needed for translocation probably reflects the involvement of additional factors that adapt the sorcin–protein partner interaction to a particular cellular environment. In cardiac cells, for example, sorcin translocation is substantially affected by β_1-adrenergic stimulation (authors' unpublished data), a process not noted in smooth muscle cells. Also, we cannot rule out that sorcin binds with higher Ca^{2+} affinity to protein partners other than RyR2.

RyRs are classical generators of Ca^{2+}-induced Ca^{2+} release (CICR) in a variety of excitable and non-excitable cells (Fill & Copello, 2002; Kamishima & Quayle, 2003), a process with inherently positive feedback that, unrestricted, tends to be an explosive mechanism of Ca^{2+} release (Stern, 1992). Smooth muscle cells, like cardiac cells, display finely controlled CICR despite organized distribution of RyRs along the periphery of the cell. Using conservative automated colocalization parameters in our isolated smooth muscle cells, up to ~50% of sorcin was found in areas populated by RyRs (Fig. 6). Under more stringent threshold setting, however, such as applied to cardiac cells, only ~30% of sorcin pixels colocalized with RyRs (not shown). Even then, the patchy and subcellular localization of this small but substantial pool of sorcin resembled the non-homogeneous and peripheral distribution of sarcoplasmic reticulum Ca^{2+}-ATPase (SERCA) pumps (Shmygol & Wray, 2004) and BK_{Ca} channels (Ohi *et al.* 2001) that have been found in close spatial relationship with VDCC and RyR clusters (Lesh *et al.* 1998; Moore *et al.* 2004). It is plausible, then, that CICR may be reigned in by the highly localized regulation of RyRs in the spatially segregated regions of the smooth muscle cell where VDCCs, SERCA pumps and BK_{Ca} channels are found, and that at least a portion of the sorcin pool influences the functional output of this interacting protein supra-complex. The demonstrated biochemical (Figs 4–6) and functional (Fig. 7) interaction of sorcin with at least one of these proteins (RyR2) supports this notion. The larger and broadly dispersed pool of cytosolic sorcin could also participate in CICR quenching if translocation to peripheral regions was fast enough to allow interaction with activated RyRs.

This report is also the first account of a successful permeabilization procedure for vascular myocytes that allows complete replacement of the cytosolic milieu with an internal solution containing Ca^{2+} buffers of variable strength. This technique allowed us not only to explore the effect of Ca^{2+} diffusion and quenching on the properties of Ca^{2+} sparks, but also to introduce a ~22 kDa Ca^{2+}-binding protein with a putative role as a modulator of intracellular Ca^{2+} signalling. Upon permeabilization, Ca^{2+} spark frequency substantially increased (Fig. 7 and Table 1), indicating that our internal solution lacked factor(s) that restrain RyR activity in intact vascular myocytes. This phenomenon occurred in cardiac cells also (Farrell *et al.* 2003), and in both cell types was restrained by perfusion of sorcin directly onto Ca^{2+} release sites. However, although

this observation provided support for a role of sorcin in modulating RyRs *in vivo*, it did not establish sorcin as the sole modifier of Ca^{2+} sparks in permeabilized *versus* intact cells. Ca^{2+} spark frequency did not return to normal values after perfusion of sorcin, and other alterations brought about by permeabilization were actually accentuated by sorcin. For example, Ca^{2+} spark amplitude decreased with permeabilization and sorcin exaggerated this reduction (Table 1). Löhn *et al.* (2000) demonstrated that dextrin depletion of caveolae (infoldings of the surface membrane, some in close apposition to junctional SR) in VSMCs modified the frequency, amplitude and spatial size of Ca^{2+} sparks. Since caveolae depletion by dextrin occurs in the absence of permeabilization, the phenomenon responsible for modification of Ca^{2+} sparks must be related to disruption of the structural relationship between triggers (dihydropyridine receptors) and effectors (RyR2) of Ca^{2+} sparks, as postulated by Löhn *et al.* (2000). Thus, permeabilization not only appears to wash out normal cytosolic modulators of Ca^{2+} release, but probably disrupts the microarchitecture surrounding the RyRs on which other Ca^{2+} spark properties depend. This was supported by the fact that EGTA, by simulating physical barriers for Ca^{2+} diffusion and buffering, 'corrected' spark properties in permeabilized cells in a manner proportional to its concentration. This artefact of permeabilization notwithstanding, the technique offered a powerful approach for the assessment of acute effects of proteins with intracellular targets.

Modification of Ca^{2+} spark properties by sorcin offered an opportunity to gain insight into the mechanism of action of this protein on RyRs and the role played by Ca^{2+} on the sorcin–RyR interaction. The Ca^{2+} spark frequency reflects the open probability of RyRs at rest and is set by the input of negative and positive modulators of RyR activity (Stern & Cheng, 2004). Perfusion of sorcin onto permeabilized cells tended to decrease spark frequency, but this effect was not nearly as robust as sorcin's ability to decrease Ca^{2+} spark amplitude, duration and spatial spread (Fig. 7 and Table 1). The latter three parameters are indexes of the *magnitude* of Ca^{2+} release by the cluster of RyRs generating the spark, the *time* the cluster remains open once it is triggered to open, and the *recruitment* by CICR of neighbouring RyR clusters along the line of scanning, respectively (Shtifman *et al.* 2002; Stern & Cheng, 2004). Sorcin's modification of these parameters falls remarkably in line with its proposed role in smooth muscle cells: at resting $[Ca^{2+}]$, sorcin is less likely to interact with its binding partners because the 'shielding' of its hydrophobic residues produces a soluble protein (Fig. 3). Spark frequency is thus almost impervious to sorcin because the sorcin–RyR interaction would not be promoted at low $[Ca^{2+}]$. However, once the spark is generated, Ca^{2+} bursts around the release sites would 'activate' sorcin (promote interaction with target proteins), which would then quench Ca^{2+} sparks by silencing a fraction of the RyRs generating the spark (decreased amplitude and duration), and by decreasing the probability of spark propagation to neighbouring RyR clusters (decreased width). The association rate of sorcin with RyR2 demonstrated in single channel experiments ($\leq$ 15 ms, Farrell *et al.* 2003) is faster than the fastest parameter of Ca^{2+} sparks (the rise time, which is $\sim$20–95 ms in smooth muscle cells; Jaggar *et al.* 2000) and supports the notion that sorcin would be able to sense the brief, localized Ca^{2+} elevations and engage in a productive interaction with RyRs before or at the peak of the Ca^{2+} spark.

In summary, sorcin density, strategic localization and demonstrated capacity to associate with RyRs place this Ca^{2+}-binding protein in a privileged position to modulate RyR activity in smooth muscle cells. The attenuation of spontaneous Ca^{2+} sparks by sorcin confirms a role for this protein in Ca^{2+} signalling and suggests it acts as a potential modulator of vascular tone in smooth muscle.

References

Collier ML, Ji G, Wang Y & Kotlikoff MI (2000). Calcium-induced calcium release in smooth muscle: loose coupling between the action potential and calcium release. *J General Physiol* **115**, 653–662.

Eghbali M, Toro L & Stefani E (2003). Diminished surface clustering and increased perinuclear accumulation of large conductance Ca^{2+}-activated K^+ channel in mouse myometrium with pregnancy. *J Biol Chem* **278**, 45311–45317.

Farrell EF, Antaramian A, Rueda A, Gómez AM & Valdivia HH (2003). Sorcin inhibits calcium release and modulates excitation-contraction coupling in the heart. *J Biol Chem* **278**, 34660–34666.

Fill M & Copello JA (2002). Ryanodine receptor calcium release channels. *Physiol Rev* **82**, 893–922.

Frank KF, Bolck B, Ding Z, Krause D, Hattebuhr N, Malik A, Brixius K, Hajjar RJ, Schrader J & Schwinger RH (2005). Overexpression of sorcin enhances cardiac contractility in vivo and in vitro. *J Mol Cell Cardiol* **38**, 607–615.

Gollasch M, Löhn M, Fürstenau M, Nelson MT, Luft FC & Haller H (2000). Ca^{2+} channels, 'quantized' Ca^{2+} release, and differentiation of myocytes in the cardiovascular system. *J Hypertens* **18**, 989–998.

Gollasch M, Wellman GC, Knot HJ, Jaggar JH, Damon DH, Bonev AD & Nelson MT (1998). Ontogeny of local sarcoplasmic reticulum Ca^{2+} signals in cerebral arteries: Ca^{2+} sparks as elementary physiological events. *Circ Res* **83**, 1104–1114.

Herrmann-Frank A, Darling E & Meissner G (1991). Functional characterization of the Ca^{2+}-gated Ca^{2+} release channel of vascular smooth muscle sarcoplasmic reticulum. *Pflugers Arch* **418**, 353–359.

Jaggar JH, Porter VA, Lederer WJ & Nelson MT (2000). Calcium sparks in smooth muscle. *Am J Physiol* **278**, C235–C256.

Jaggar JH, Wellman GC, Heppner TJ, Porter VA, Perez GJ, Gollasch M, Kleppisch T, Rubart M, Stevenson AS, Lederer WJ, Knot HJ, Bonev AD & Nelson MT (1998). Ca^{2+} channels, ryanodine receptors and Ca^{2+}-activated K^+ channels: a functional unit for regulating arterial tone. *Acta Physiol Scand* **164**, 577–587.

Ji G, Feldman ME, Greene KS, Sorrentino V, Xin HB & Kotlikoff MI (2004). RYR2 proteins contribute to the formation of Ca^{2+} sparks in smooth muscle. *J General Physiol* **123**, 377–386.

Kamishima T & Quayle JM (2003). Ca^{2+}-induced Ca^{2+} release in cardiac and smooth muscle cells. *Biochem Soc Trans* **31**, 943–946.

Kotlikoff MI (2003). Calcium-induced calcium release in smooth muscle: the case for loose coupling. *Prog Biophys Mol Biol* **83**, 171–191.

Lesh RE, Nixon GF, Fleischer S, Airey JA, Somlyo AP & Somlyo AV (1998). Localization of ryanodine receptors in smooth muscle. *Circ Res* **82**, 175–185.

Löhn M, Fürstenau M, Sagach V, Elger M, Schulze W, Luft FC, Haller H & Gollasch M (2000). Ignition of calcium sparks in arterial and cardiac muscle through caveolae. *Circ Res* **87**, 1034–1039.

Lokuta AJ, Meyers MB, Sander PR, Fishman GI & Valdivia HH (1997). Modulation of cardiac ryanodine receptors by sorcin. *J Biol Chem* **272**, 25333–25338.

Lukyanenko V & Györke S (1999). Ca^{2+} sparks and Ca^{2+} waves in saponin-permeabilized rat ventricular myocytes. *J Physiol* **521**, 575–585.

Matsumoto T, Hisamatsu Y, Ohkusa T, Inoue N, Sato T, Suzuki S, Ikeda Y & Matsuzaki M (2005). Sorcin interacts with sarcoplasmic reticulum Ca^{2+}-ATPase and modulates excitation-contraction coupling in the heart. *Basic Res Cardiol* **100**, 250–262.

Mella M, Colotti G, Zamparelli C, Verzili D, Ilari A & Chiancone E (2003). Information transfer in the penta-EF-hand protein sorcin does not operate via the canonical structural/functional pairing. A study with site-specific mutants. *J Biol Chem* **278**, 24921–24928.

Meyers MB, Fischer A, Sun YJ, Lopes CM, Rohacs T, Nakamura TY, Zhou YY, Lee PC, Altschuld RA, McCune SA, Coetzee WA & Fishman GI (2003). Sorcin regulates excitation-contraction coupling in the heart. *J Biol Chem* **278**, 28865–28871.

Meyers MB, Pickel VM, Sheu SS, Sharma VK, Scotto KW & Fishman GI (1995*b*). Association of sorcin with the cardiac ryanodine receptor. *J Biol Chem* **270**, 26411–26418.

Meyers MB, Schneider KA, Spengler BA, Chang TD & Biedler JL (1987). Sorcin (V19), a soluble acidic calcium-binding protein overproduced in multidrug-resistant cells. Identification of the protein by anti-sorcin antibody. *Biochem Pharmacol* **36**, 2373–2380.

Meyers MB, Spengler BA, Chang TD, Melera PW & Biedler JL (1985). Gene amplification-associated cytogenetic aberrations and protein changes in vincristine-resistant Chinese hamster, mouse, and human cells. *J Cell Biol* **100**, 588–597.

Meyers MB, Zamparelli C, Verzili D, Dicker AP, Blanck TJ & Chiancone E (1995*a*). Calcium-dependent translocation of sorcin to membranes: functional relevance in contractile tissue. *FEBS Lett* **357**, 230–234.

Moore ED, Voigt T, Kobayashi YM, Isenberg G, Fay FS, Gallitelli MF & Franzini-Armstrong C (2004). Organization of Ca^{2+} release units in excitable smooth muscle of the guinea-pig urinary bladder. *Biophys J* **87**, 1836–1847.

Nelson MT, Cheng H, Rubart M, Santana LF, Bonev AD, Knot HJ & Lederer WJ (1995). Relaxation of arterial smooth muscle by calcium sparks. *Science* **270**, 633–637.

Ohi Y, Yamamura H, Nagano N, Ohya S, Muraki K, Watanabe M & Imaizumi Y (2001). Local Ca^{2+} transients and distribution of BK channels and ryanodine receptors in smooth muscle cells of guinea-pig vas deferens and urinary bladder. *J Physiol* **534**, 313–326.

Pérez GJ, Bonev AD, Patlak JB & Nelson MT (1999). Functional coupling of ryanodine receptors to KCa channels in smooth muscle cells from rat cerebral arteries. *J General Physiol* **113**, 229–238.

Peskoff A & Langer GA (1998). Calcium concentration and movement in the ventricular cardiac cell during an excitation-contraction cycle. *Biophys J* **74**, 153–174.

Powell T, Matsuoka S, Sarai N & Noma A (2004). Intracellular Ca^{2+} dynamics and sarcomere length in single ventricular myocytes. *Cell Calcium* **35**, 535–542.

Rodriguez P, Bhogal MS & Colyer J (2003). Stoichiometric phosphorylation of cardiac ryanodine receptor on serine 2809 by calmodulin-dependent kinase II and protein kinase A. *J Biol Chem* **278**, 38593–38600.

Rueda A, Scherman JA & Valdivia HH (2005). Sorcin modulates spatio-temporal properties of calcium sparks in permeabilized smooth muscle cells. *Biophys J* **88**, 632a.

Seidler T, Miller SL, Loughrey CM, Kania A, Burow A, Kettlewell S, Teucher N, Wagner S, Kogler H, Meyers MB, Hasenfuss G & Smith GL (2003). Effects of adenovirus-mediated sorcin overexpression on excitation-contraction coupling in isolated rabbit cardiomyocytes. *Circ Res* **93**, 132–139.

Shmygol A & Wray S (2004). Functional architecture of the SR calcium store in uterine smooth muscle. *Cell Calcium* **35**, 501–508.

Shtifman A, Ward CW, Yamamoto T, Wang J, Olbinski B, Valdivia HH, Ikemoto N & Schneider MF (2002). Interdomain interactions within ryanodine receptors regulate Ca^{2+} spark frequency in skeletal muscle. *J General Physiol* **119**, 15–32.

Stern MD (1992). Theory of excitation-contraction coupling in cardiac muscle. *Biophys J* **63**, 497–517.

Stern MD & Cheng H (2004). Putting out the fire: what terminates calcium-induced calcium release in cardiac muscle? *Cell Calcium* **35**, 591–601.

Suarez J, Belke DD, Gloss B, Dieterle T, McDonough PM, Kim YK, Brunton LL & Dillmann WH (2004). In vivo adenoviral transfer of sorcin reverses cardiac contractile abnormalities of diabetic cardiomyopathy. *Am J Physiol* **286**, H68–H75.

Valdivia HH (1998). Modulation of intracellular Ca^{2+} levels in the heart by sorcin and FKBP12, two accessory proteins of ryanodine receptors. *Trends Pharmacol Sci* **19**, 479–482.

Yang XR, Lin MJ, Yip KP, Jeyakumar LH, Fleischer S, Leung GP & Sham JS (2005). Multiple ryanodine receptor subtypes and heterogeneous ryanodine receptor-gated Ca^{2+} stores in pulmonary arterial smooth muscle cells. *Am J Physiol* **289**, L338–L348.

Zamparelli C, Ilari A, Verzili D, Vecchini P & Chiancone E (1997). Calcium- and pH-linked oligomerization of sorcin causing translocation from cytosol to membranes. *FEBS Lett* **409**, 1–6.

Acknowledgements

We wish to thank Beth Altschafl for providing us with control ventricular myocytes for the immunostainings experiments and her critical reading of this manuscript and Joseph A. Scherman and Craig Weber for help with the immunoprecipitation experiments. This work was supported by NIH grants HL55438 and HL76826 (to H.H.V.), and Consejo National de Ciencia y Tecnología and American Heart Association fellowships to A.R.